





## Article

# Predicting Crop Evapotranspiration under Non-Standard Conditions Using Machine Learning Algorithms, a Case Study for *Vitis vinifera* L. cv Tempranillo

Ricardo Egpto <sup>1,\*</sup> , Arturo Aquino <sup>2</sup> , Joaquim Costa <sup>3</sup>  and José Manuel Andújar <sup>2</sup> 

<sup>1</sup> INIAV, I.P.—Instituto Nacional de Investigação Agrária e Veterinária, Pólo de Inovação de Dois Portos, Quinta da Almoíña, 2565-191 Dois Portos, Portugal

<sup>2</sup> CITES, Centro de Investigación en Tecnología, Energía y Sostenibilidad, Universidad de Huelva, La Rábida, Palos de la Frontera, 21819 Huelva, Spain; arturo.aquino@diesia.uhu.es (A.A.); andujar@diesia.uhu.es (J.M.A.)

<sup>3</sup> LEAF, Linking Landscape, Environment, Agriculture and Food, Instituto Superior de Agronomia, Universidade de Lisboa, 1349-017 Lisboa, Portugal; miguelcosta@isa.ulisboa.pt

\* Correspondence: ricardo.egpto@iniav.pt

**Abstract:** This study focuses on assessing the accuracy of supervised machine learning regression algorithms (MLAs) in predicting actual crop evapotranspiration (ET<sub>c act</sub>) for a deficit irrigated vineyard of *Vitis vinifera* cv. Tempranillo, influenced by a typical Mediterranean climate. The standard approach of using the Food and Agriculture Organization (FAO) crop evapotranspiration under standard conditions (FAO-56 Kc-ET<sub>0</sub>) to estimate ET<sub>c act</sub> for irrigation purposes faces limitations in row-based, sparse, and drip irrigated crops with large, exposed soil areas, due to data requirements and potential shortcomings. One significant challenge is the accurate estimation of the basal crop coefficient (K<sub>cb</sub>), which can be influenced by incorrect estimations of the effective transpiring leaf area and surface resistance. The research results demonstrate that the tested MLAs can accurately estimate ET<sub>c act</sub> for the vineyard with minimal errors. The Root-Mean-Square Error (RMSE) values were found to be in the range of 0.019 to 0.030 mm·h<sup>-1</sup>. Additionally, the obtained MLAs reduced data requirements, which suggests their feasibility to be used to optimize sustainable irrigation management in vineyards and other row crops. The positive outcomes of the study highlight the potential advantages of employing MLAs for precise and efficient estimation of crop evapotranspiration, leading to improved water management practices in vineyards. This could promote the adoption of more sustainable and resource-efficient irrigation strategies, particularly in regions with Mediterranean climates.

**Keywords:** grapevine; vineyard irrigation; actual crop evapotranspiration; machine learning algorithms; decision support systems



**Citation:** Egpto, R.; Aquino, A.; Costa, J.; Andújar, J.M. Predicting Crop Evapotranspiration under Non-Standard Conditions Using Machine Learning Algorithms, a Case Study for *Vitis vinifera* L. cv Tempranillo. *Agronomy* **2023**, *13*, 2463. <https://doi.org/10.3390/agronomy13102463>

Academic Editor: Junliang Fan

Received: 1 August 2023

Revised: 12 September 2023

Accepted: 19 September 2023

Published: 23 September 2023



**Copyright:** © 2023 by the authors. Licensee MDPI, Basel, Switzerland. This article is an open access article distributed under the terms and conditions of the Creative Commons Attribution (CC BY) license (<https://creativecommons.org/licenses/by/4.0/>).

## 1. Introduction

Viticulture is a vital socio-economic activity for Mediterranean countries, but it faces significant challenges due to climate change and extreme weather conditions. More severe droughts and higher temperatures are expected [1], leading to increased evaporative demand and reduced water availability for irrigation. In this context, efficient irrigation management is crucial for optimizing yield and berry composition in vineyards. Such a scenario brings new challenges to Mediterranean viticulture, as irrigation emerges as an adaptation strategy aimed at optimizing yield while improving ripening and berry composition [2,3].

Grape ripening is a critical phenological phase that greatly influences berry composition at harvest time. Moderate water stress during this period benefits grapevine water-use efficiency and grape quality [2]. Accurate quantification of this condition requires monitoring actual crop evapotranspiration (ET<sub>c act</sub>), which allows for the implementation of

efficient irrigation management schemes. To ensure optimal plant water status, irrigation protocols must be based on accurate knowledge of weather, soil, and plant variables. Nevertheless, there is some debate among plant physiologists and micrometeorologists regarding the factors contributing to plant water loss through transpiration. Plant physiologists emphasize the role of stomata in this process [4–6], while micrometeorologists focus on the high energy required for water evaporation [7].

Several methods to estimate evapotranspiration (ET), incorporating various factors from soil to vegetation and based on weather variables, have been developed [8]. Some are derived from the Penman–Monteith equation, which describes the ET process considering the soil and air moisture, mass transfer, and the energy required for the process [7]. The Food and Agriculture Organization (FAO) recommends crop evapotranspiration under standard conditions (FAO-56 Kc-ET<sub>0</sub>) as the standard approach for defining and calculating reference ET (ET<sub>0</sub>). Since ET<sub>0</sub> reflects the weather-related effects on water use by a reference crop [9,10], in order to be applicable to different crops, the method needs to scale ET<sub>0</sub> by a crop coefficient (Kc), which accounts for the physical and physiological differences from the reference crop, their impact on ET<sub>0</sub>, and their variability during the growing season [9]. Several simplifications were incorporated into the Kc coefficients, including plant transpiration and soil evaporation [11]. To avoid incorrect estimation of crop ET (ETc) in orchards and sparse crops with drip irrigation and large exposed soil areas, the FAO-56 Kc-ET<sub>0</sub> method was adapted to separate plant and soil components of Kc, the basal crop (Kcb) and the soil evaporation coefficient (Ke) [9]. However, for crop species with tight stomatal control of water loss and regulation of leaf water potential, such as grapevine, literature has reported major accuracy limitations in using the FAO-56 Kc-ET<sub>0</sub> method [11–15]. These inaccuracies are mainly related to the surface resistance and incorrect estimation of Kcb [16–18]. In fact, the procedure for the practical estimation of the ETc act, must take into account the effective transpiring leaf area, and additionally include auxiliary sub-models for aerodynamics and surface conductance, which must be parameterized for each new measurement, location, and condition [15,19–22].

To overcome the limitations of the FAO-56 Kc-ET<sub>0</sub> method, alternative approaches, such as employing machine learning regression algorithms (MLA) can be considered [23,24]. Indeed, MLAs have the capacity to map input-dependent variables to output-independent ones by learning patterns from training datasets with known pairs of input-output data [25]. Previous studies in the literature describe the use of MLA approaches to estimate ET<sub>0</sub>, but to the best of our knowledge, none of them relates to farm scale calculation of the ETc act for grapevines [24,26–29].

This research assesses the performance of eight state-of-the-art supervised machine learning regression algorithms (MLA), using three main atmospheric variables (net radiation—R<sub>n</sub>, wind speed—U, and vapor pressure deficit—VPD) and a plant variable (stomatal conductance to water vapor—g<sub>sw</sub>), to predict ETc act as key information for designing optimal irrigation management systems in vineyards. To assess the accuracy of the algorithms, ETc act estimates by MLA are compared to the accuracy of the ETc act computed by the FAO-56 Kc-ET<sub>0</sub> method, using the actual crop ET recorded by the Eddy covariance tower flux installed in the field as an external validation variable.

The findings suggest that MLA models can be effective in estimating the ETc act and optimizing irrigation management in vineyards. These models can continuously improve and expand their knowledge by incorporating new data from agronomic campaigns. The application of MLA in arid climates can significantly benefit viticulture in Mediterranean regions.

## 2. Materials and Methods

### 2.1. Experimental Layout

The trials were carried out in a commercial vineyard (Herdade do Esporão) in Reguengos de Monsaraz, Alentejo wine region, southern Portugal (lat. 38°23′55.00″ N; long. 7°32′46.00″ W). Specifically, a 17-year-old commercial vineyard of the red *Vitis vinifera* cv

Tempranillo (syn. Aragonez), grafted on 1103 Paulsen rootstock, was chosen for the study. The vines are 1.5 m within and 3.0 m between rows (2220 vines/ha), north-south oriented, trained to vertical shoot positioning, and spur-pruned on a bilateral Royat cordon system. All vines were pruned evenly, with 15–16 buds per vine. A Eutric Cambisol (CM) with a depth of 1.0 m and a silty-clay texture was found, with a pH ranging from 7.0 to 7.6, a low organic matter content, and a high content of phosphorus and potassium. Standard cultural practices in the region were followed, and the vines were irrigated weekly with drip irrigation, using  $2.4 \text{ L}\cdot\text{h}^{-1}$ , 1.0 m spaced emitters, in accordance with owners' practices.

For the study, 20 adult and healthy vines were randomly selected from two adjacent rows, with 10 vines per row. This criterion of narrow sample selection increases confidence in the coherence of the measurements, as it ensures an optimal data acquisition procedure under conditions of low temporal and spatial variability within each measurement, without compromising the variability observed in the field. This experimental design also allowed for the assessment of solar radiation effects, as both sides of the canopy (east and west) were studied under contrasting incident radiation.

The field trial, detailed in Section 2.2.1, was carried out during the ripening period in 2019 (20 and 22 July) and 2020 (24, 29 and 31 August), from 8 a.m. to 7 p.m.

## 2.2. Field and Reference Measurements

### 2.2.1. Field Measurements

Wind speed ( $U$ ) was measured with a 3D sonic anemometer (Gill Windmaster Pro, Gill Instruments Limited, Hampshire, UK). To avoid gust peaks, the wind speed was recalculated using a 300-s running average over the incoming wind signal [30] and corrected by applying Equation (1) to wind speed measured 3 m above the ground surface [9]:

$$U = U_z \cdot \frac{4.87}{\ln(67.8z - 5.42)} \quad (1)$$

where  $U$  is the wind speed ( $\text{m}\cdot\text{s}^{-1}$ ) measured at 2 m above the ground surface,  $U_z$  is the wind speed ( $\text{m}\cdot\text{s}^{-1}$ ) measured in  $z$  m above the ground surface, and  $z$  is the height above the ground surface (m) at which the wind speed is measured. Air temperature ( $T_{\text{air}}$ ) and relative humidity (RH) were recorded using a thermohygrometer (CS215-PWS Campbell Scientific, Logan, UT, USA) placed 2 m above the soil surface. Net radiation ( $R_n$ ) was measured with a net radiometer (NR2, Delta-T Devices, Cambridge, UK), installed above the top of the canopy. Soil heat flux ( $G$ ) was measured with six heat flux plates (Hukseflux HFP01, Hukseflux Thermal Sensors, Delft, The Netherlands), placed at 5 mm depth, one under the canopy, and the others 0.5 m apart, perpendicular to the vine row and covering all the inter-row. Soil heat flux data are presented as the average of all six measurements. Soil and meteorological sensors were connected to a datalogger (CR1000, Campbell Scientific, Logan, UT, USA) and data was collected every minute and averaged every five minutes. Plant water status was assessed by pre-dawn leaf water potential ( $\Psi_{\text{PD}}$ ) measurements on each sampling date using a Scholander-type pressure chamber. Water vapor gas exchange was also monitored by measuring stomatal conductance to water vapor ( $g_{\text{sw}}$ ) on adult leaves from each side of the canopy, from 8 a.m. to 7 p.m., using a steady state porometer (LI-1600, LI-COR, Lincoln, NE, USA). A summary of the field measurements is shown in Table 1.

### 2.2.2. Characterization of the Climate and Grapevine Water Status

The study zone's climate is Mediterranean, with hot and dry summers and mild rainy winters. Accumulated rainfall from October to August ranged from 341 to 466 mm in 2019 and 2020, respectively (Table 2).

**Table 1.** Summary of field measurements and instrumentation.

Measurement	Periodicity and Data Integration	Units	Source
Stomatal conductance to water vapor ( $g_{sw}$ )	Hourly from 8 a.m. to 7 p.m.	$m \cdot s^{-1}$	Steady-state porometer (Model LI-1600, LI-COR, Lincoln, NE, USA)
Air temperature ( $T_{air}$ ) Air relative humidity (RH)	Every minute and averaged every 5 min	$^{\circ}C$ %	Temperature and relative humidity probe, model CS215-PWS (Campbell Scientific, Logan, UT, USA) connected to a datalogger (CR1000, Campbell Scientific, Inc.)
Wind speed (U)	Every 1/10 s and averaged every minute	$m \cdot s^{-1}$	3D sonic anemometer (model Gill Windmaster Pro, Gill Instruments Limited, Hampshire, UK)
Net radiation (Rn)	Every minute and averaged every 5 min	$W \cdot m^{-2}$	Net radiometer, model NR2, (Delta-T Devices, Cambridge, UK) connected to a datalogger (CR1000, Campbell Scientific, Inc., Logan, UT, USA)
Soil heat flux (G)	Every minute and averaged every 5 min	$W \cdot m^{-2}$	Hukseflux heat flux plate, model HFP01 (Hukseflux Thermal Sensors, Delft, The Netherlands) connected to a datalogger (CR1000, Campbell Scientific, Inc., Logan, UT, USA)
Vapor pressure deficit (VPD)	Every minute and averaged every 5 min	kPa	$VPD = e_s - e_a \quad (2)$ $e_a = e^{\circ}(T) \cdot \frac{RH}{100} \quad (3)$ $e^{\circ}(T) = 0.6108 \cdot \exp\left(\frac{17.27 \times T}{T + 237.3}\right) \quad (4)$ $e_s = \frac{e^{\circ}(T_{min}) + e^{\circ}(T_{max})}{2} \quad (5)$ where ( $e_s$ ) is the saturation and ( $e_a$ ) is the actual vapor pressure, for a given period [9]

**Table 2.** Characterization of rainfall patterns. Accumulated rainfall during grapevine dormancy, from October (Oct) to December (Dec) of the previous year's vintage (year ( $i - 1$ )), dormancy to flowering (January–May), and berry development to grape ripening (June (Jun) to August (Aug)) of the harvest year (year ( $i$ )) and the cumulative rainfall from October of the previous year to August.

	Rainfall (mm)				
	Year ( $i - 1$ )		Year ( $i$ )		Accum
	Year ( $i$ )	Oct–Dec	Jan–May	Jun–Aug	
2019		204.4	133.6	3.4	341.4
2020		226.0	239.0	1.2	466.2

Hourly averaged net solar radiation above the canopy ( $R_n$ ,  $W \cdot m^{-2}$ ), soil heat flux ( $G$ ,  $W \cdot m^{-2}$ ), air temperature ( $T_{air}$ ,  $^{\circ}C$ ), wind speed ( $U$ ,  $m \cdot s^{-1}$ ), and air vapor pressure deficit (VPD, kPa), during the experimental period and measured on the experimental plot, are shown in Figure 1. All measurements were taken under clear-sky conditions.  $T_{air}$  and VPD followed a similar daily pattern. In the afternoon, the VPD was always above 3 kPa and reached 4.5 to 5 kPa between 5 p.m. and 6 p.m. The wind speed,  $U$ , was moderate, with a maximum of  $4.4 m \cdot s^{-1}$ . The vineyard row orientation and the apparent daily course of the sun influenced the soil heat flux. The  $G$  increased from the early hours of the day until 2 p.m., when it almost reached its maximum value, and decreased after 3 p.m. when  $R_n$  decreased.  $R_n$ , soil  $G$ ,  $T_{air}$ , and VPD showed a similar diurnal pattern during all measurement periods.

Predawn leaf water potential ( $\Psi_{PD}$ ) varied between  $-0.4$  and  $-0.6$  MPa, corresponding to a condition of moderate to severe stress in grapevine, considered adequate to produce high-standard wines [2,31] (Table 3). A moderate recovery in  $\Psi_{PD}$  was observed after each irrigation event, with an increase of more than 0.1 MPa, (e.g., on 22 August 2019, and on 24 and 29 July 2020).

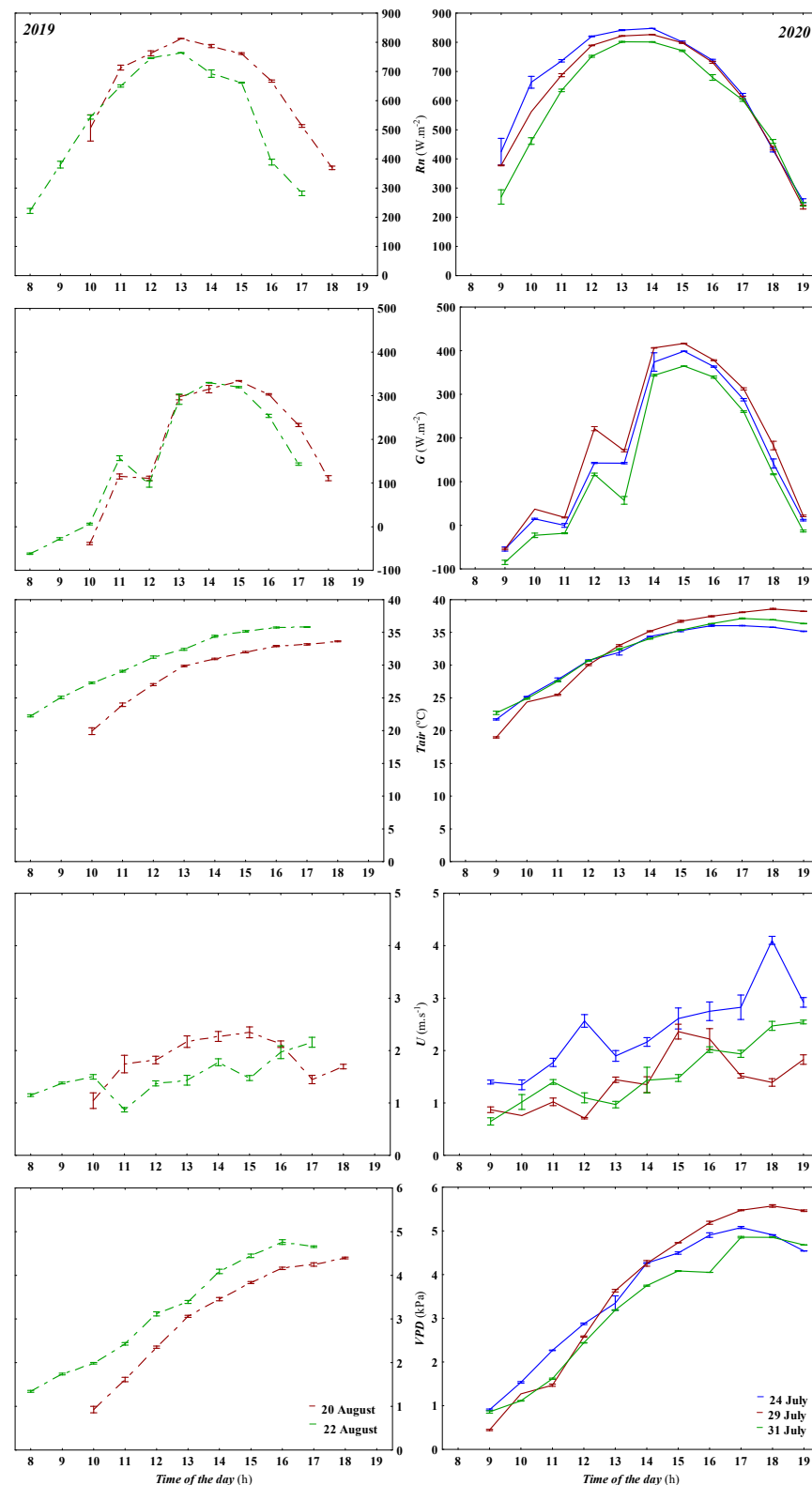


**Figure 1.** Atmospheric and Soil Variable Patterns on the Measurement Days. The figure illustrates the measurements of net solar radiation above the canopy ( $R_n$ ,  $W \cdot m^{-2}$ ), Soil heat flux ( $G$ ,  $W \cdot m^{-2}$ ), air temperature ( $T_{air}$ ,  $^{\circ}C$ ), wind speed ( $U$ ,  $m \cdot s^{-1}$ ), and air vapor pressure deficit ( $VPD$ ,  $kPa$ ) measured on 20 and 22 August 2019 and 24, 29 and 31 July 2020 on the experimental plot is presented. The values represent means, and the vertical bars indicate the standard error of the mean plots ( $n = 12$ ).

**Table 3.** Predawn leaf water potential ( $\Psi_{PD}$ ) of grapevines on the measurement days. The table displays measurements of predawn leaf water potential ( $\Psi_{PD}$ ) of grapevines on specific measurement days. Measurements were conducted on 20 August (before irrigation) and 22 August 2019 (after irrigation) at 4–5 a.m., as well as on the 24 July (after irrigation), 29 July 2020 (before irrigation), and 31 July 2020 (after irrigation). The data is presented as the mean (Avg) and standard error of the mean (SE) of five replicates per day.

DAY	$\Psi_{PD}$ (MPa)	
	Avg	SE
20 August 2019 (before irrigation)	−0.60	0.012
22 August 2019 (after irrigation)	−0.52	0.021
24 July 2020 (after irrigation)	−0.42	0.020
29 July 2020 (before irrigation)	−0.55	0.017
31 July 2020 (after irrigation)	−0.47	0.017

### 2.2.3. Reference Actual Crop Evapotranspiration Measurements

An EC system installed on the experimental plot was used to record actual crop evapotranspiration ( $ET_c$  act meas) simultaneously with U. A part of the collected data was used as a target variable in the model training phase and a part as an external validation dataset. The EC system consisted of a fast response, 0.1 Hz, open path  $CO_2/H_2O$  analyzer (LI-6500 DS, LI-COR Inc., Lincoln, NE, USA) and a 3D sonic anemometer (Gill Windmaster Pro, Gill Instruments Limited, Hampshire, UK) connected to a Smartflux 3 system (LI-COR Inc., Lincoln, NE, USA). The sonic anemometer and the open path  $CO_2/H_2O$  analyzer were installed at a height of 3.0 m above the ground surface, over the top of the canopy. A fetch of at least 300 m, facing the prevailing north winds and covering the experimental field ensured that all fluxes within the area of interest were measured. The quality of the recorded data was tested and analyzed with the EddyPro software v7.0.6 (LI-COR Inc., Lincoln, NE, USA). The measurements enabled us to record the registered actual evapotranspiration ( $ET_c$  act meas) at a high temporal resolution, every 1/10 s.

More than 90% of the daily data flux of the dataset analyzed here had an energy balance closure greater than 0.95. Consequently, the uncertainty of the measured  $ET_c$  act meas values was less than 5%, which corresponded to an  $ET_c$  act meas measurement uncertainty of less than  $0.002 \text{ mm h}^{-1}$  on the hourly flux determination of 90% of the data.

Despite the significant differences between the  $ET_c$  act meas recorded before and after irrigation days, similar patterns were found in the  $ET_c$  act meas recorded before irrigation and in the  $ET_c$  act meas recorded after irrigation (Figure 2). Irrespective of the irrigation difference, the  $ET_c$  act meas increased exponentially from the early morning hours, reaching its peak between 11 a.m. and 12 p.m. In 2020, when the grapevines were less stressed after irrigation (Table 3), the maximum  $ET_c$  act meas reading was recorded at 1 p.m., when the air VPD reached 3.5 MPa, and decreased towards the end of the day, regardless of the energy available for water evaporation. In both years, prior to irrigation, and under more severe water stress conditions, the maximum  $ET_c$  act meas reading was registered at 11 a.m. and was maintained at a similar level for an extended period, only decreasing after 5 p.m. to 6 p.m. (Figure 2). These results are consistent with the strong regulation of  $g_{sw}$  on grapevine transpiration [4], and the large contribution of plant transpiration compared to soil evaporation to total evapotranspiration in vineyards. While before irrigation,  $ET_c$  act meas ranged from 0.06 to less than  $0.2 \text{ mm} \cdot \text{h}^{-1}$ , the recorded  $ET_c$  act meas after irrigation was on average 1.3 to 1.4 times higher, thus suggesting larger stomata opening and greater water loss through transpiration.

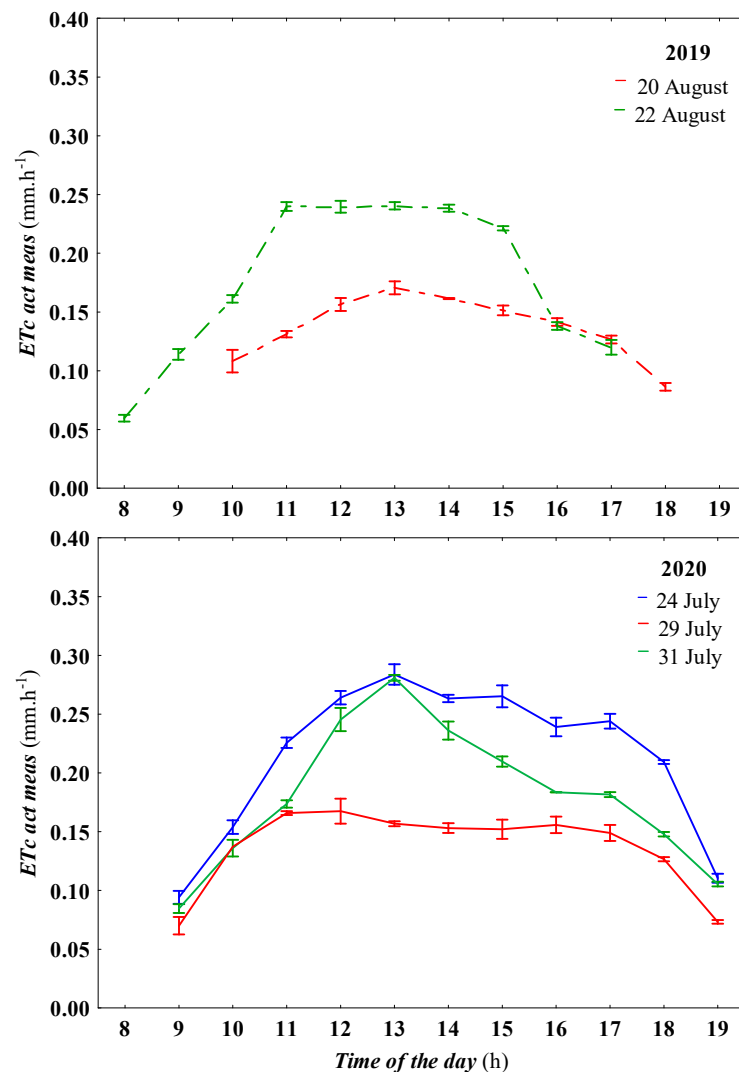


**Figure 2.** Actual crop evapotranspiration ( $ET_c$  act meas) measured in the experimental plot. The figure displays the actual crop evapotranspiration ( $ET_c$  act meas) measured in the experimental plot using an Eddy covariance flux tower. Measurements were taken on the 20 and 22 August 2019, before and after irrigation, respectively, as well as on the 24 July, after irrigation, 29 July, before irrigation, and after irrigation on 31 July 2020. The values represent means, and the vertical bars indicate the standard error of the mean plots.

### 2.3. Developed Methodology

#### 2.3.1. Data Processing and Analysis

In order to estimate actual crop evapotranspiration, under non-standard conditions ( $ET_c$  act est), from weather and plant variables using machine learning techniques, the initial field measurement data underwent a transformation to create a suitable data structure for processing and analysis. The original data were structured into a nine-dimensional vector composed of the seven measured variables ( $g_{sw}$ ,  $ET_c$  act meas,  $T_{air}$ , RH, U,  $R_n$ , and G) and two derived variables ( $R_n - G$  and VPD), with 600 measurements per variable. VPD was calculated using  $T_{air}$  and RH as described in Equations (2)–(5) (Table 1). To train the machine learning models (MLA) to estimate actual crop evapotranspiration,  $ET_c$  act est, the  $ET_c$  act meas recorded in the experimental plot was used as the label/dependent variable (target), and the variables  $g_{sw}$ , VPD,  $R_n$ , G, U, and  $T_{air}$  were initially considered as predictors, subject to the results of the pre-processing analysis. The predictor variables were selected from the crop and meteorological variables with the greatest influence on  $ET_c$  act according to the literature.

Data pre-processing included outlier analysis, variable correlation analysis, and data structuring into an internal training and testing set, and an external validation dataset. Outliers were identified by the interquartile range (IQR) method with a cut-off of  $1.5 \times \text{IQR}$ . Scores that fell below  $1.5 \times \text{IQR} - Q1$  (the 1st or 25% quartile) or above  $1.5 \times \text{IQR} + Q3$  (the 3rd or 75% quartile) were considered as outliers and removed from the dataset. To avoid multicollinearity of the model, the correlation of the variables was analyzed by a Pearson product-moment correlation test. Variables not correlating below  $-0.6$  or above a threshold of  $0.6$  were selected as good candidates for ETc act predictors. Consequently, the variable Tair was removed based on this criterion. After removing the outliers and discarding the variable, the data were randomly split into three datasets: A training and testing dataset containing 40% of the 2019 and 2020 data, and two validation datasets, one containing the remaining 2019 data, and the other containing the remaining 2020 data (Figure 3). The three datasets were configured to maintain similar data patterns (Table 4).

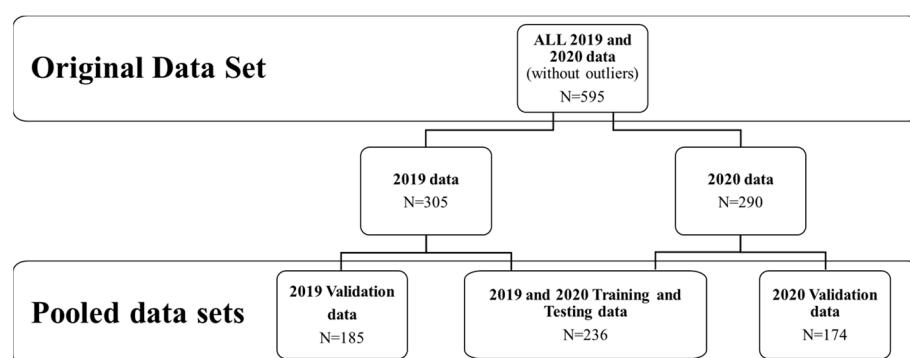


**Figure 3.** Data structure. The original data was divided into three final datasets: a training and testing dataset containing 40% of all data from the years 2019 and 2020, and two external validation datasets containing the remaining data from the years 2019 and 2020.

### 2.3.2. Modeling Vineyard Actual Evapotranspiration under Non-Standard Conditions

The pooled training dataset (Figure 3) was used to train and fit a set of supervised machine learning regression models to predict ETc act pred, employing a five-fold cross-validation scheme to protect against overfitting. The selected model predictors, as detailed above, were the daily course of net radiation ( $R_n$ ,  $W \cdot m^{-2}$ ), soil heat flux ( $G$ ,  $W \cdot m^{-2}$ ), air vapor pressure deficit (VPD, kPa), wind speed ( $U$ ,  $m \cdot s^{-1}$ ) measured above the canopy, as well as the stomatal conductance to water vapor ( $g_{sw}$ ,  $m \cdot s^{-1}$ ). The pooled training dataset, ETc act meas data, recorded in the field (Figure 3), was used as the target variable. For modeling purposes, the units of  $g_{sw}$  were converted to  $m \cdot s^{-1}$  using the molar density of the air ( $mol \cdot m^{-3}$ ), and  $R_n$  after subtracting  $G$  to determine the energy available for crop ET processes.

Accordingly, a set of supervised machine learning models was developed, using Matlab R2021b (The Mathworks Inc., Natick, MA, USA), which included:

- A non-parametric kernel-based probabilistic model (Gaussian process regression model—GPR), using either an exponential kernel function or a squared exponential kernel function;
- A support vector machine (SVM) regression model using either a linear kernel function, a quadratic kernel function, a cubic kernel function, or a medium Gaussian kernel function;
- An ensemble of regression trees (ERT), either using least-squares boosting regression trees learners or using bootstrap-aggregating (bagging) regression trees learners.



**Table 4.** Model predictors and characterization of response variables. The table provides variable characterization for each pooled dataset (training, testing, and validation). It includes stomatal conductance to water vapor ( $g_{sw}$ ), net radiation above the canopy minus soil heat flux ( $Rn - G$ ), wind speed ( $U$ ), air vapor pressure deficit above the canopy ( $VPD$ ), and crop evapotranspiration measured by the Eddy covariance method under non-standard conditions ( $ETc$  act meas). The data are characterized by the total number of cases ( $N$ ), the mean of the variable (Mean), the minimum (Min) and maximum (Max) values, the standard deviation (SD), and the respective coefficient of variation (CV, %).

Variable	Training and Testing Data Set					
	Valid N	Mean	Min	Max	SD	CV
$g_{sw}$ ( $\text{mol}\cdot\text{H}_2\text{O m}^{-2}\cdot\text{s}^{-1}$ )	236	0.081	0.004	0.254	0.041	50.5
$Rn - G$ ( $\text{W}\cdot\text{m}^{-2}$ )	236	425.0	56.3	779.7	159.0	37.4
$U$ ( $\text{m}\cdot\text{s}^{-1}$ )	236	1.69	0.57	4.16	0.72	42.2
$VPD$ (kPa)	236	3.36	0.46	5.62	1.43	42.4
$ETc$ act meas ( $\text{mm}\cdot\text{h}^{-1}$ )	236	0.167	0.020	0.388	0.066	39.5
Variable	2019 Validation Dataset					
	Valid N	Mean	Min	Max	SD	CV
$g_{sw}$ ( $\text{mol}\cdot\text{H}_2\text{O m}^{-2}\cdot\text{s}^{-1}$ )	174	0.085	0.014	0.249	0.050	58.6
$Rn - G$ ( $\text{W}\cdot\text{m}^{-2}$ )	174	455.5	189.1	767.5	159.1	34.9
$U$ ( $\text{m}\cdot\text{s}^{-1}$ )	174	1.81	0.52	4.45	0.83	45.6
$VPD$ (kPa)	174	3.47	0.41	5.70	1.58	45.6
$ETc$ act meas ( $\text{mm}\cdot\text{h}^{-1}$ )	174	0.176	0.025	0.369	0.072	41.0
Variable	2020 Validation Dataset					
	Valid N	Mean	Min	Max	SD	CV
$g_{sw}$ ( $\text{mol}\cdot\text{H}_2\text{O m}^{-2}\cdot\text{s}^{-1}$ )	185	0.079	0.004	0.149	0.030	38.0
$Rn - G$ ( $\text{W}\cdot\text{m}^{-2}$ )	185	403.7	82.0	665.4	145.1	35.9
$U$ ( $\text{m}\cdot\text{s}^{-1}$ )	185	1.59	0.73	3.05	0.49	31.2
$VPD$ (kPa)	185	3.17	0.76	5.22	1.26	39.6
$ETc$ act meas ( $\text{mm}\cdot\text{h}^{-1}$ )	185	0.157	0.043	0.280	0.058	37.3

#### 2.4. Methodology to Evaluate the Predictive Accuracy of MLA Models in Estimating Actual Crop Evapotranspiration

To assess the predictive accuracy of the proposed MLA models, the actual crop evapotranspiration predicted by the models,  $ETc$  act pred, was compared to the  $ETc$  act meas measurements recorded in the field by the Eddy covariance method. To better examine the performance of the proposed models, we also compared the predictive accuracy of  $ETc$  act estimated by the FAO-56 Kc- $ET_0$  method with the values from the same dataset of  $ETc$  act meas recorded in the field using the Eddy covariance method. Finally, the accuracy of MLA models for predicting  $ETc$  act was verified by comparison with the accuracy of the recommended standard method FAO-56 Kc- $ET_0$  for estimating  $ETc$  act.

##### 2.4.1. Predictive Accuracy of MLA Models to Estimate Actual Crop Evapotranspiration

The accuracy of the MLA proposals for predicting  $ETc$  act was verified by comparing the fitted values of all models with the  $ETc$  act meas measures recorded in the field by the Eddy covariance method. The predictive accuracy of the MLA models was evaluated according to the method described in Section 2.4.3.

##### 2.4.2. Predictive Accuracy of the FAO-56 Kc- $ET_0$ Model to Estimate Actual Crop Evapotranspiration

The accuracy of the predicted  $ETc$  act using the recommended standard method FAO-56 Kc- $ET_0$  was compared to the  $ETc$  act meas measurements recorded in the field by the Eddy covariance method.

To predict ET<sub>c</sub> act using the FAO-56 K<sub>c</sub>-ET<sub>0</sub> standard method, ET<sub>0</sub> was first calculated according to the method proposed by [9] using data from the farm's meteorological station. A detailed description of the FAO-56 K<sub>c</sub>-ET<sub>0</sub> method can be found in the work by [9]. In this study, the dual crop coefficient K<sub>c</sub> approach was employed to assess crop evapotranspiration (ET<sub>c</sub>). This approach involves splitting K<sub>c</sub> into two factors that separately describe the components soil evaporation (K<sub>e</sub>) and grapevine transpiration (K<sub>cb</sub>). The basal crop coefficient (K<sub>cb</sub>) was estimated by the Normalized Differential Vegetation Index (NDVI) obtained from Sentinel 2 imagery time-series with a spatial resolution of 10 m, following the model presented in [32] (Equation (6)).

$$K_{cb} = 1.44 \times NDVI - 0.10 \quad (6)$$

The model presented in [32] was developed for a vineyard with the same cultivar and rootstock, and a similar climate and crop management, showing a high coefficient of determination ( $R^2 = 0.96$ ). Thus, Equation (6) was selected to estimate K<sub>cb</sub> from the NDVI measured in the experimental plot.

As the grapevines in the study were subjected to some stress, a stress coefficient (K<sub>s</sub>) was applied to K<sub>cb</sub> to assess ET<sub>c</sub> act according to the FAO-56 K<sub>c</sub>-ET<sub>0</sub> methodology, following Equation (7):

$$ET_c \text{ act} = (K_e + K_s \times K_{cb}) \times ET_0 \quad (7)$$

The calculation of K<sub>s</sub> was based on Equation (8), as described in [32]:

$$K_s = 1.217 \times e^{(1.444 \times \Psi_{PD})} \quad (8)$$

The predictive accuracy of the FAO-56 K<sub>c</sub>-ET<sub>0</sub> standard method was evaluated according to the method described in Section 2.4.3.

#### 2.4.3. Comparative Analysis of the Predictive Accuracy of MLA Models and the FAO-56 K<sub>c</sub>-ET<sub>0</sub> Method for Estimating Actual Crop Evapotranspiration

The models' predictive accuracy was assessed for the pairs model—dataset by examining the coefficient of determination ( $R^2$ ) of the trained models and comparing the goodness of fit measures of the simulated vs. observed ET<sub>c</sub> act. For this purpose, we used the Root-Mean-Square-Error (RMSE), which is defined as follows:

$$RMSE = \sqrt{\frac{\sum_{i=1}^n (\hat{y}_i - y_i)^2}{n}} \quad (9)$$

where  $\hat{y}_i$  and  $y_i$  are the predicted and measured actual crop ET, respectively, for the  $i$ -th segment of the dataset and  $n$  is the number of ET<sub>c</sub> act measurements used in each dataset.

To avoid the differences in ET<sub>c</sub> act between different datasets, the relative error ( $|E|$ ) was calculated and expressed as a percentage, from the expression:

$$|E| = \frac{|\sum_{i=1}^n (\hat{y}_i - y_i)|}{\sum_{i=1}^n y_i} \times 100 \quad (10)$$

### 3. Results and Discussion

#### 3.1. Characterization and Correlations of Actual Crop Evapotranspiration Predictors

Figure 4 shows the correlation between all variables trained as predictors of actual crop evapotranspiration (ET<sub>c</sub> act) before data was split into datasets. Since air temperature (T<sub>air</sub>) showed a positive and significant correlation with air VPD ( $R = 0.97$ ,  $p < 0.001$ ), T<sub>air</sub> was not used as a predictor of ET<sub>c</sub> act to avoid multicollinearity. All variables correlated positively and significantly ( $p < 0.001$ ) with the target variable (ET<sub>c</sub> act meas). With the exception of Rn-G, the energy available for the ET process, which showed a correlation coefficient (R) value with ET<sub>c</sub> act meas twice that of the other predictors, all others correlate in a similar order of magnitude. None of the predictors per se explained more than 40% of

the variability of the ET<sub>c act meas</sub>, thus suggesting that non-linear relationships between predictors and the ET<sub>c act meas</sub> may be involved, and/or the interaction between the variables are the main contributors to the observed variability.

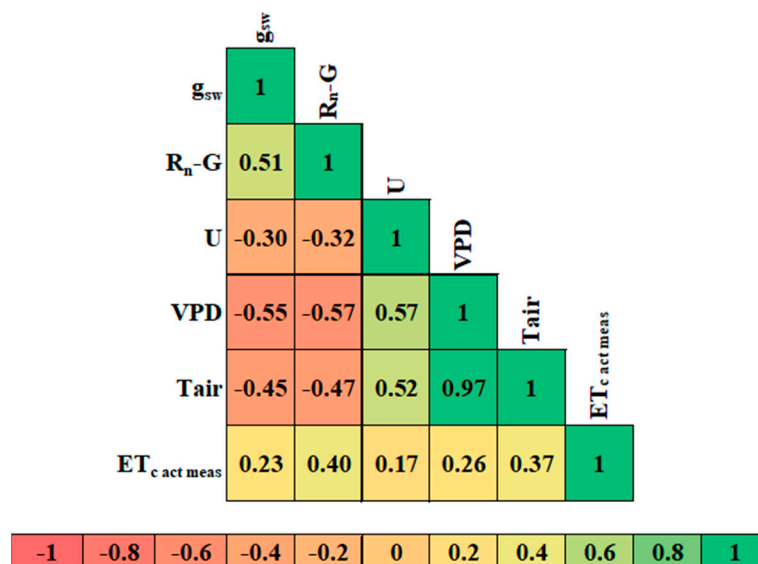


**Figure 4.** Correlogram Showing Pearson Product-Moment Correlation Coefficients. The figure displays the Pearson product-moment correlation coefficients between pairs of variables selected as predictor candidates for actual crop evapotranspiration (ET<sub>c act</sub>). The variables include meteorological variables such as Rn-G (the energy available for crop evapotranspiration processes, calculated as the net solar radiation above the canopy (Rn) minus the soil heat flux (G)), U (the wind speed above the canopy), VPD (the air vapor pressure deficit), and Tair (the air temperature). Additionally, the grapevine variable g<sub>sw</sub> (stomatal conductance to water vapor) and field-measured actual crop evapotranspiration (ET<sub>c act meas</sub>) are included in the correlation analysis. All correlation coefficients are significantly different from zero ( $p < 0.001$ ). Correlations of similar magnitude are depicted with the same color, according to the color code shown below.

Table 4 shows the characterization of the datasets used for training and testing, as well as for external validation of the MLA approach and FAO-56 Kc-ET<sub>0</sub> models. The table shows considerable variability within each variable across all datasets, as indicated by the coefficient of variation (CV). This variability can be attributed to how the different variables changed throughout the day. Despite the variability, the mean and the amplitude of data variability, represented by the maximum (Max) and minimum (Min) values, as well as the standard deviation (SD) of each variable (both predictor and target variables), were found to be similar between datasets (Table 4).

### 3.2. Evaluation of MLA Models in Estimating Actual Crop Evapotranspiration

Table 5 shows the fitted supervised machine learning (MLA) models that were trained and tested to estimate ET<sub>c act</sub> using the variables Rn, G, U, VPD, and g<sub>sw</sub> as predictors. In the testing phase, all trained models achieved a high and significant coefficient of determination (R<sup>2</sup>), thus indicating high efficiency in predicting the ET<sub>c act</sub>. The poorer model was the SVM approach, using a linear kernel function, which yielded an R<sup>2</sup> score of 0.746. The two ERT approaches, the SVM model, using a medium Gaussian kernel function, and the GPR, using an exponential kernel function, showed the best performance in predicting the ET<sub>c act</sub>, with R<sup>2</sup> values between 0.910 and 0.992. The high and significant R<sup>2</sup> of all MLA regression models (Table 5) indicates that the selected variables (g<sub>sw</sub>, Rn-G, U, and VPD) account for a very high proportion of the observed ET<sub>c act</sub> variability, suggesting that they are robust explanatory variables of the ET<sub>c act</sub>.

**Table 5.** Fitted Machine Learning Algorithms for actual vineyard evapotranspiration under non-standard conditions (ETc act). The table presents the results of fitted Machine Learning Algorithms for actual vineyard evapotranspiration under non-standard conditions (ETc act) using the pooled dataset for training and testing. The data was obtained from the years 2019 and 2020, based on actual vineyard evapotranspiration measured by the Eddy covariance method in the field ( $n = 236$ ). The values of the coefficient of determination ( $R^2$ ) for all the algorithms are significant ( $p < 0.001$ ).

Machine Learning Algorithms	$R^2$
GPR Exponential kernel function	0.992
GPR Squared Exponential kernel function	0.899
SVM Linear kernel function	0.746
SVM Quadratic kernel function	0.819
SVM Cubic kernel function	0.878
SVM Medium Gaussian kernel function	0.925
Ensemble Boosted Trees	0.934
Ensemble Bagged Trees	0.910

Table 6 presents the goodness-of-fit measures for the MLA approaches used to estimate the ETc act using the validation dataset with the variables Rn, G, U, VPD, and  $g_{sw}$ . The results of the validation phase were consistent with those of training and testing. Except for the SVM implementing a linear kernel function, the model validation process demonstrated the high accuracy of the remaining MLA models for predicting the ETc act. The results showed a correlation (R) between observed and fitted values greater than 0.880 and a maximum root mean square error (RMSE) of  $0.032 \text{ mm}\cdot\text{h}^{-1}$ , which is below the minimum ETc act value recorded in both years (as shown in Table 6 and Figure 5).

**Table 6.** Statistical indicators of goodness-of-fit measures of the supervised machine learning regression algorithms. The table presents statistical indicators of goodness-of-fit measures for estimating vineyard evapotranspiration under non-standard conditions (ETc act) using supervised machine learning regression algorithms. The data validation was performed with two independent datasets: observed (field recorded) vineyard evapotranspiration under non-standard conditions (ETc act meas) and model-estimated vineyard evapotranspiration under non-standard conditions (ETc act est). The datasets are from the years 2019 ( $n = 185$ ) and 2020 ( $n = 174$ ). The goodness-of-fit measures included are root mean square error (RMSE) and relative error (|E|).

Machine Learning Algorithms	Year Dataset	RMSE ( $\text{mm}\cdot\text{h}^{-1}$ )	E  (%)
GPR Exponential kernel function	2019	0.019	4.6
	2020	0.026	1.8
GPR Squared Exponential kernel function	2019	0.020	6.3
	2020	0.027	0.9
SVM Linear kernel function	2019	0.026	0.9
	2020	0.042	1.1
SVM Quadratic kernel function	2019	0.022	1.9
	2020	0.032	3.5
SVM Cubic kernel function	2019	0.022	4.9
	2020	0.031	1.5
SVM Medium Gaussian kernel function	2019	0.019	5.4
	2020	0.029	0.7
Ensemble Boosted Trees	2019	0.020	0.2
	2020	0.030	5.1
Ensemble Bagged Trees	2019	0.020	4.5
	2020	0.030	1.3

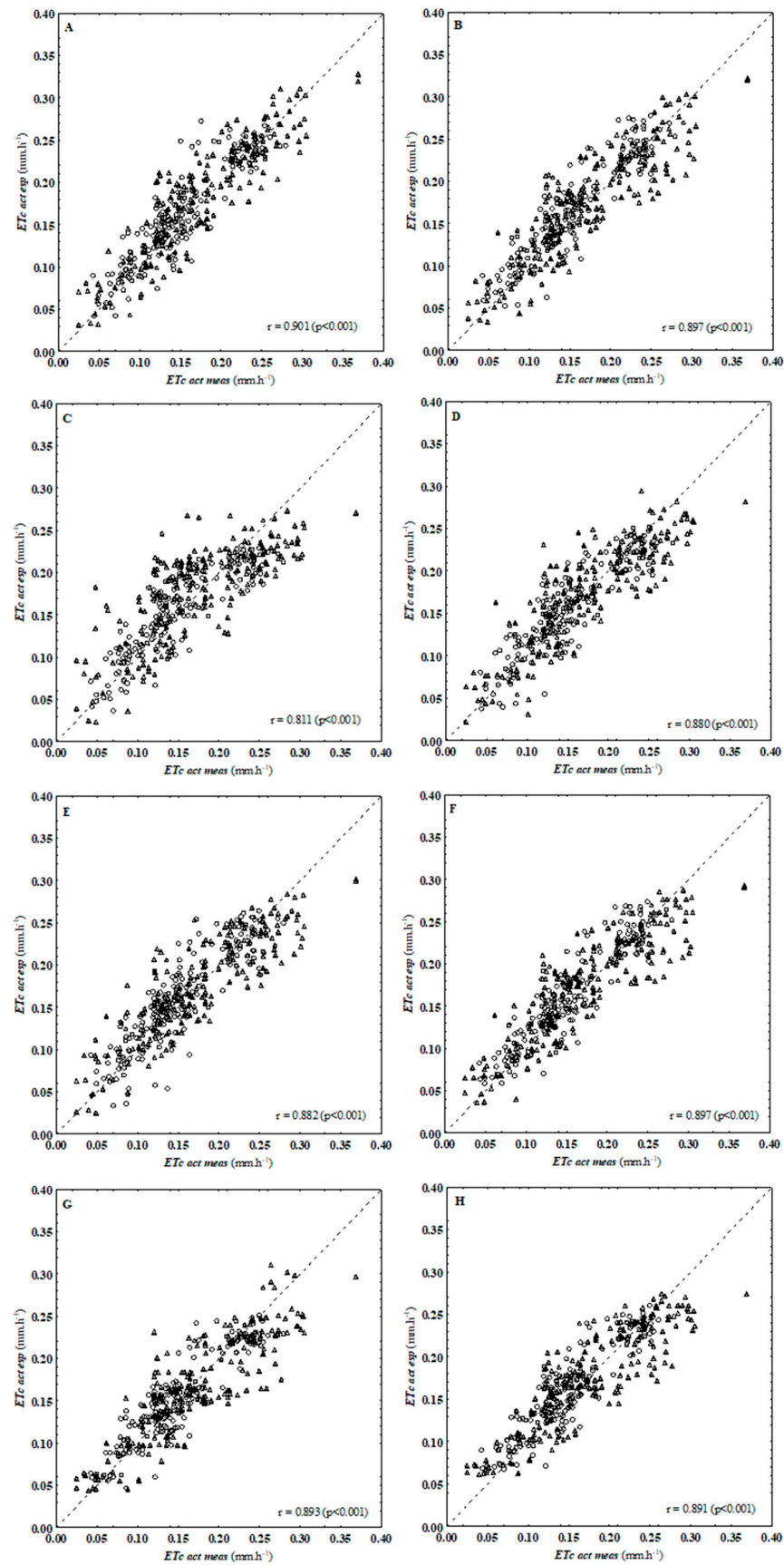


**Figure 5.** Relationship between observed and estimated crop evapotranspiration. This figure illustrates the relationship between the observed crop evapotranspiration (ETc act meas, mm·h<sup>-1</sup>),

recorded with an Eddy covariance flux tower, and the actual crop evapotranspiration ( $ET_c$  act est,  $\text{mm}\cdot\text{h}^{-1}$ ) estimated by different supervised machine learning algorithms. Each subfigure shows a specific algorithm used for estimation. (A) recorded  $ET_c$  act meas value versus  $ET_c$  act est value estimated by a GPR using an exponential kernel function. (B) relationship estimated by a GPR algorithm using a squared exponential kernel function. (C) relationship estimated by an SVM algorithm with a linear kernel function. (D) relationship estimated by an SVM algorithm with a quadratic kernel function, while (E) relationship estimated by an SVM algorithm with a cubic kernel function. (F) relationship estimated by an SVM algorithm with a medium Gaussian kernel function. (G) relationship estimated by an Ensemble boost tree algorithm, and (H) relationship estimated by an Ensemble bagged tree algorithm. The data validation samples from 2019 are represented with circles ( $n = 185$ ), and data from 2020 are represented with triangles ( $n = 174$ ). The dotted line in each subfigure represents the 1:1 line, indicating perfect alignment between the observed and estimated values.

The analysis of the goodness-of-fit measures of the models in Table 6 confirmed that the MLA with a linear transformation had the poorest performance in estimating the  $ET_c$  act. However, the MLA models tested with the year 2019 and 2020 independent validation datasets demonstrated high accuracy potential in predicting the  $ET_c$  act, with  $R^2$  values ranging between 0.629 (SVM using a linear kernel function, and the 2020 validation dataset) and 0.915 (SVM using a medium Gaussian kernel function, and the 2019 validation dataset). The relative error ( $|E|$ ) of the predictions made with the 2019 validation dataset was in the  $[0.2, 6.3]$  interval, while with the 2020 dataset, the range was  $[0.7, 5.1]$ , both expressed in percentage. Overall, the MLA models exhibited strong predictive capabilities for estimating  $ET_c$  act, as evidenced by their high  $R^2$  values and relatively low errors.

All algorithms explained more than 80% of the  $ET_c$  act variability present in the validation dataset. The GPR using an exponential and a squared exponential kernel function, both ERT, using either least squares boosting or bootstrap aggregation methods and the SVM with a medium Gaussian kernel function, showed the best accuracy in estimating the  $ET_c$  act. These algorithms explain between 80 and 90% of the variability of the  $ET_c$  act measured in the field while exhibiting an RMSE in the range of 0.019 to 0.030  $\text{mm}\cdot\text{h}^{-1}$ . Excluding the SVM using a linear transformation, the MLA algorithms, using plant and weather variables, showed a remarkable ability to learn the inner relations between  $ET_c$  act meas,  $R_n$ ,  $G$ ,  $U$ , and  $VPD$ , by predicting the actual vineyard ET variability with high accuracy. Similar results were obtained by other authors [24,26,27,33–35] for other crops.

### 3.3. Evaluation of FAO-56 $K_c$ - $ET_0$ Method to Estimate Actual Crop Evapotranspiration

Figure 6 depicts the scatter plot representing the relationship between the observed actual crop evapotranspiration ( $ET_c$  act meas) recorded with the Eddy covariance method and the estimated actual crop evapotranspiration ( $ET_c$  act est) obtained through the application of the FAO 56  $K_c$ - $ET_0$  method (fitted values). The results reveal a noteworthy and statistically significant correlation ( $R = 0.858$ ,  $p < 0.001$ ) between the observed and fitted data. However, it is evident that the variability increases as the magnitude of the observed values rises, as illustrated in Figure 6. Moreover, the FAO 56  $K_c$ - $ET_0$  method exhibits a tendency to overestimate the actual crop evapotranspiration values, which is consistent with findings in other studies concerning olive orchards [36] and peach orchards [16]. Consequently, the goodness-of-fit measures indicate an RMSE of 0.059  $\text{mm}\cdot\text{h}^{-1}$ , a value 1.3 to 2.9 times higher than the minimum  $ET_c$  act recorded in the field using the Eddy covariance method. Furthermore, the relative error ( $|E| = 26.5\%$ ) is relatively high, indicating certain weaknesses of the FAO-56  $K_c$ - $ET_0$  method in accurately predicting  $ET_c$  act in sparse vegetation crops like vineyards. This observation underscores the method's limitations in simulating soil resistance and vine stomatal conductance under more stressful conditions, as investigated in this study. The observed limitations of the FAO-56  $K_c$ - $ET_0$  method in

accurately estimating  $ET_c$  act in vineyards are consistent with previous literature, including studies by [15,16,19,22,36,37].

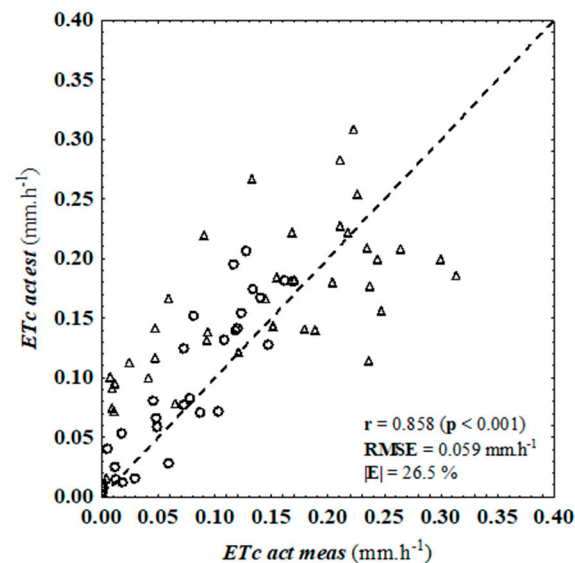


**Figure 6.** Relationship between observed and estimated actual crop evapotranspiration. The figure illustrates the relationship between the observed actual crop evapotranspiration ( $ET_c$  act meas) recorded using the Eddy covariance flux tower, and the actual crop evapotranspiration estimated ( $ET_c$  act est) with the FAO-56 Kc- $ET_0$  method. The coefficient of determination ( $R^2$ ) and goodness-of-fit measures from data validation with two independent datasets of observed vineyard evapotranspiration under non-standard conditions ( $ET_c$  act meas) and estimated actual crop evapotranspiration ( $ET_c$  act est) with FAO 56 Kc- $ET_0$  method from the year 2019 ( $n = 48$ , circles) and 2020 ( $n = 72$ , triangles) are presented in the figure. The Goodness-of-fit measures include root mean square error (RMSE) and relative error ( $|E|$ ). The dotted line in the figure represents the 1:1 line, indicating perfect agreement between the observed and estimated values.

### 3.4. Comparison of the Prediction Accuracy of MLA and FAO-56 Kc- $ET_0$ Method to Estimate Actual Crop Evapotranspiration

With the exception of SVM implementing a linear kernel, all MLA proposals demonstrated superior performance in predicting  $ET_c$  act compared to the FAO-56 Kc- $ET_0$  method. The scatterplots depicting the relationship between the observed  $ET_c$  act values (recorded with the EC method) and the estimated  $ET_c$  act est values (obtained through MLA) showed a close alignment with the 1:1 line, indicating a good fit of all MLA models (see Figure 5). During the validation process, the MLA models exhibited a very high and statistically significant coefficient of determination ( $R^2$ ) between the simulated and observed values. Moreover, the intercept and slope of the MLA fitted values were very close to 0 and 1, respectively, further confirming the accuracy of the predictions. In contrast, when compared to the FAO-56 Kc- $ET_0$  method, only the SVM with a linear kernel exhibited a lower  $R^2$  and a less satisfactory fit to the observed data. This outcome suggests that the SVM with a linear kernel might not be as effective as the other MLA models in accurately estimating  $ET_c$  act under the conditions considered in this study.

The comparison of accuracy between models, using the external validation dataset, clearly indicates that the MLA models outperform the FAO-56 Kc- $ET_0$  method. The MLA models' fitted values demonstrated significantly smaller errors (as measured by RMSE and  $|E|$ ) compared to the FAO-56 Kc- $ET_0$  method. Specifically, the scatterplots between the observed and the FAO-56 Kc- $ET_0$  fitted values showed an RMSE that was 1.65 to 1.98 times less accurate, in 2019 and 2020, respectively, when compared to the worst MLA proposal (SVM with a linear kernel function). Moreover, the FAO-56 Kc- $ET_0$  method was found to be 2.2 to 2.8 times less accurate, in 2019 and 2020, respectively, when compared to the

best MLA models, namely the GPR with an exponential kernel function, and the SVM with a medium Gaussian kernel function. In terms of prediction capacity, all MLA models exhibited higher accuracy compared to the FAO-56 Kc-ET<sub>0</sub> model. The absolute value of the error ( $|E|$ ) in the MLA predictions was more than 6.8 times lower than the values predicted by the FAO-56 Kc-ET<sub>0</sub> model, as shown in Table 7.

**Table 7.** Comparison of prediction accuracy to estimate actual crop evapotranspiration recorded in the field. The table provides a comparison of prediction accuracy to estimate actual crop evapotranspiration recorded in the field using the Eddy covariance method. It includes results from the FAO-56 Kc-ET<sub>0</sub> and the two best machine learning algorithms: GPR (Gaussian process regression) using an exponential kernel function, and SVM (Support vector machine) using a medium Gaussian kernel function. Prediction accuracy measures include the coefficient of determination ( $R^2$ ) of the trained models, and the goodness-of-fit measures from the data validation process (root mean square error—RMSE and relative error— $|E|$ ).

	$R^2$	RMSE (mm·h <sup>-1</sup> )		$ E $ (%)	
		2019	2020	2019	2020
FAO-56 Kc-ET <sub>0</sub>	0.736	0.043	0.083	37.0	22.6
GPR Exponential kernel function	0.805	0.019	0.026	4.6	1.8
SVM Medium Gaussian kernel function	0.812	0.019	0.030	5.4	0.7

These findings further strengthen the superiority of MLA models in accurately estimating actual crop evapotranspiration compared to the traditional FAO-56 Kc-ET<sub>0</sub> method. The significant reduction in errors, as indicated by RMSE and  $|E|$  values, highlights the enhanced predictive capabilities of MLA models in this study.

#### 4. Conclusions

The present work demonstrates that machine learning regression algorithms, when provided with  $g_{sw}$ ,  $G$ , and three meteorological variables ( $R_n$ ,  $U$ , and  $VPD$ ), can accurately predict the ETc act. The five best-performing algorithms explain more than 89% of the measured variability in ETc act recorded in the field, with RMSE values below 0.03 mm·h<sup>-1</sup>. The results showcase the MLA's capacity to estimate the ETc act with a simple parameterization and lower computational requirements compared to the traditional FAO-56 Kc-ET<sub>0</sub> method while retaining robustness in calculations.

Furthermore, the findings highlight the limitations of the FAO-56 Kc-ET<sub>0</sub> method in accurately predicting ETc act for grapevines under deficit irrigation, where vine stomatal significantly impacts water usage and soil surface water evaporation is limited. In contrast, the presented MLA models, which incorporate  $g_{sw}$  as input knowledge, proved to be accurate in predicting ETc act under such conditions.

The study shows that the MLA models are well suited for application in semi-automated or automated field data analysis for predicting vineyard ETc act. Their ability to continuously process new data in near real time, retrain the algorithm, and adapt to new data patterns and associations can enhance prediction accuracy and support more efficient irrigation practices.

Additionally, the use of machine learning algorithms for monitoring the ETc act based on grapevine and atmospheric parameters can provide valuable insights for decision support systems aimed at optimizing vineyard irrigation management. However, further optimization is required concerning the amount of available data and consideration of climatic conditions.

In conclusion, the study demonstrates the efficacy of MLA algorithms in accurately estimating vineyard ETc act, making them a promising approach for water management in grapevine cultivation. Nonetheless, future research should focus on refining the models with respect to data availability and varying climatic conditions.



**Author Contributions:** Conceptualization, R.E.; methodology, R.E.; formal analysis, R.E.; investigation, R.E.; resources, A.A. and J.M.A.; data curation, R.E.; writing—original draft preparation, R.E.; writing—review and editing, R.E., A.A., J.C. and J.M.A.; supervision, A.A. and J.M.A. All authors have read and agreed to the published version of the manuscript.

**Funding:** This work was supported by Fundação para a Ciência e a Tecnologia (Portugal) through the R&D Unit “GREEN-IT—Bioresources for Sustainability” (UIDB/04551/2020 and UIDP/04551/2020).

**Data Availability Statement:** Data available on request. The data presented in this study are available on request from the corresponding author.

**Acknowledgments:** We acknowledge FCT Research Unit “GREEN-IT—Bioresources for Sustainability” (UIDB/04551/2020 and UIDP/04551/2020) for financial support. We also thank the support of the research units CITES, Centro de Investigación en Tecnología, Energía y Sostenibilidad, Universidad de Huelva, and LEAF (UID/AGR/04129/2019). We also address our acknowledgements to Herdade do Esporão (Reguengos de Monsaraz, Alentejo, PT) and Rui Flores for their contribution to field management of the experimental vineyard.

**Conflicts of Interest:** The authors declare no conflict of interest.

## References

1. Intergovernmental Panel on Climate Change (IPCC). AR6 Synthesis Report: Climate Change. 2022. Available online: [https://www.ipcc.ch/site/assets/uploads/2018/02/WGIIAR5-Chap3\\_FINAL.pdf](https://www.ipcc.ch/site/assets/uploads/2018/02/WGIIAR5-Chap3_FINAL.pdf) (accessed on 30 May 2023).
2. Chaves, M.M.; Zarrouk, O.; Francisco, R.; Costa, J.M.; Santos, T.; Regalado, A.P.; Rodrigues, M.L.; Lopes, C.M. Grapevine under deficit irrigation: Hints from physiological and molecular data. *Ann. Bot.* **2010**, *105*, 661–676. [[CrossRef](#)] [[PubMed](#)]
3. Costa, J.M.; Vaz, M.; Escalona, J.M.; Egipto, R.; Lopes, C.M.; Medrano, H.; Chaves, M.M. Modern viticulture in Southern Europe: Vulnerabilities and strategies for adaptation to water scarcity. *Agr. Water Manag.* **2016**, *164*, 5–18. [[CrossRef](#)]
4. Chaves, M.M.; Costa, J.M.; Zarrouk, O.; Pinheiro, C.; Lopes, C.M.; Pereira, J.S. Controlling stomatal aperture in semi-arid regions—The dilemma of saving water or being cool? *Plant Sci.* **2016**, *251*, 54–64. [[CrossRef](#)] [[PubMed](#)]
5. Simonneau, T.; Lebon, E.; Coupel-Ledru, A.; Marguerit, E.; Rossedeutsch, L.; Ollat, N. Adapting plant material to face water stress in vineyards: Which physiological targets for an optimal control of plant water status? *OENO One* **2017**, *51*, 167–179. [[CrossRef](#)]
6. Levin, A.D.; Williams, L.E.; Mathews, M.A. A continuum of stomatal responses to water deficits among 17 wine grape cultivars (*Vitis vinifera*). *Funct. Plant Biol.* **2019**, *47*, 11–25. [[CrossRef](#)]
7. Monteith, J.L.; Unsworth, M. *Principles of Environmental Physics*, 4th ed.; Academic Press: Cambridge, MA, USA; Elsevier: Oxford, UK, 2013; ISBN 978-0-12-386910-4.
8. Priestley, C.H.B.; Taylor, R.J. On the assessment of surface heat flux and evaporation using large-scale parameters. *Mon. Weather Rev.* **1972**, *100*, 81–92. [[CrossRef](#)]
9. Allen, R.G.; Pereira, L.S.; Raes, D.; Smith, M. *Crop Evapotranspiration Guidelines for Computing Crop Water Requirements—FAO Irrigation and Drainage Paper 56*, 1st ed.; FAO: Rome, Italy, 1998; Available online: <http://www.fao.org/3/X0490E/X0490E00.htm> (accessed on 4 May 2023).
10. Pereira, A.R. The Priestley–Taylor parameter and the decoupling factor for estimating reference evapotranspiration. *Agr. For. Meteorol.* **2004**, *125*, 305–313. [[CrossRef](#)]
11. Pereira, L.S.; Allen, R.G.; Smith, M.; Raes, D. Crop evapotranspiration estimation with FAO56: Past and future. *Agr. Water Manag.* **2015**, *147*, 4–20. [[CrossRef](#)]
12. Shuttleworth, W.J.; Wallace, J.S. Calculating the water requirements of irrigated crops in Australia using the Matt-Shuttleworth approach. *Trans. ASABE* **2009**, *52*, 1895–1906. [[CrossRef](#)]
13. Campos, I.; Neale, C.M.U.; Calera, A.; Balbontina, C.; González-Piqueras, J. Assessing satellite-based basal crop coefficients for irrigated grapes (*Vitis vinifera* L.). *Agr. Water Manag.* **2010**, *98*, 45–54. [[CrossRef](#)]
14. Schymanski, S.J.; Or, D. Leaf-scale experiments reveal an important omission in the Penman–Monteith equation. *Hydrol. Earth Syst. Sci.* **2017**, *21*, 685–706. [[CrossRef](#)]
15. Forster, M.A.; Kim, T.D.H.; Kunz, S.; Abuseif, M.; Chulliparambil, V.R.; Srichandra, J.; Michael, R.N. Phenology and canopy conductance limit the accuracy of 20 evapotranspiration models in predicting transpiration. *Agr. For. Meteorol.* **2022**, *315*, 108824. [[CrossRef](#)]
16. Paço, T.A.; Ferreira, I.; Conceição, N. Peach orchard evapotranspiration in a sandy soil: Comparison between eddy covariance measurements and estimates by the FAO 56 approach. *Agr. Water Manag.* **2006**, *85*, 305–313. [[CrossRef](#)]
17. Picón-Toro, J.; González-Dugo, V.; Uriarte, D.; Mancha, L.A.; Testi, L. Effects of canopy size and water stress over the crop coefficient of a “Tempranillo” vineyard in south-western Spain. *Irrig. Sci.* **2012**, *30*, 419–432. [[CrossRef](#)]
18. Rallo, G.; Paço, T.A.; Paredes, P.; Puig-Sirera, À.; Massai, R.; Provenzano, G.; Pereira, L.S. Updated single and dual crop coefficients for tree and vine fruit crops. *Agr. Water Manag.* **2021**, *250*, 106645. [[CrossRef](#)]
19. Villalobos, F.J.; Orgaz, F.; Testi, L.; Fereres, E. Measurement and modeling of evapotranspiration of olive (*Olea europaea* L.) orchards. *Eur. J. Agron.* **2000**, *13*, 155–163. [[CrossRef](#)]

20. Ortega-Farias, S.; Irmak, S.; Cuenca, R.H. Special issue on evapotranspiration measurement and modeling. *Irrig. Sci.* **2009**, *28*, 1–3. [[CrossRef](#)]
21. Rana, G.; Katerji, N.; Lorenzi, F. Measurement and modelling of evapotranspiration of irrigated citrus orchard under Mediterranean conditions. *Agr. For. Meteorol.* **2021**, *128*, 199–209. [[CrossRef](#)]
22. Nyolei, D.; Diels, J.; Mbilinyi, B.; Mbungu, W.; van Griensven, A. Evapotranspiration simulation from a sparsely vegetated agricultural field in a semi-arid agro-ecosystem using Penman-Monteith models. *Agr. For. Meteorol.* **2021**, *303*, 108370. [[CrossRef](#)]
23. Sarker, I.H. Machine Learning: Algorithms, Real-World Applications and Research Directions. *Sn Comput. Sci.* **2021**, *2*, 160. [[CrossRef](#)]
24. Yong, S.L.S.; Ng, J.L.; Huang, Y.F.; Ang, C.K. Estimation of evapotranspiration with three different machine learning models and limited meteorological variables. *Agronomy* **2023**, *13*, 1048. [[CrossRef](#)]
25. Mahesh, B. Machine learning algorithms—A review. *Int. J. Sci. Res.* **2020**, *9*, 381–386.
26. Dou, X.; Yang, Y. Evapotranspiration estimation using four different machine learning approaches in different terrestrial ecosystems. *Comput. Electron. Agr.* **2018**, *148*, 95–106. [[CrossRef](#)]
27. Granata, F. Evapotranspiration evaluation models based on machine learning algorithms—A comparative study. *Agr. Water Manag.* **2019**, *217*, 303–315. [[CrossRef](#)]
28. Chen, Z.; Zhu, Z.; Jiang, H.; Sun, S. Estimating daily reference evapotranspiration based on limited meteorological data using deep learning and classical machine learning methods. *J. Hydrol.* **2020**, *591*, 125286. [[CrossRef](#)]
29. Yamaç, S.S.; Todorovic, M. Estimation of daily potato crop evapotranspiration using three different machine learning algorithms and four scenarios of available meteorological data. *Agr. Water Manag.* **2020**, *228*, 105875. [[CrossRef](#)]
30. WMO. *Guide to Instruments and Methods of Observation. Measurement of Meteorological Variables*; World Meteorological Organization: Geneva, Switzerland, 2018. Available online: [https://library.wmo.int/doc\\_num.php?explnum\\_id=10179](https://library.wmo.int/doc_num.php?explnum_id=10179) (accessed on 10 May 2023).
31. van Leeuwen, C.; Trégoat, O.; Choné, X.; Bois, B.; Pernet, D.; Gaudillère, J.-P. Vine water status is a key factor in grape ripening and vintage quality for red Bordeaux wine. How can it be assessed for vineyard management purposes? *OENO One* **2009**, *43*, 121–134. [[CrossRef](#)]
32. Ferreira, M.I. Stress Coefficients for Soil Water Balance Combined with Water Stress Indicators for Irrigation Scheduling of Woody Crops. *Horticulturae* **2017**, *3*, 38. [[CrossRef](#)]
33. Torres, A.F.; Walker, W.R.; McKee, M. Forecasting daily potential evapotranspiration using machine learning and limited climatic data. *Agr. Water Manag.* **2011**, *98*, 553–562. [[CrossRef](#)]
34. Zhang, Z.; Gong, Y.; Wang, Z. Accessible remote sensing data based reference evapotranspiration estimation modelling. *Agr. Water Manag.* **2018**, *210*, 59–69. [[CrossRef](#)]
35. Fernández-López, A.; Marín-Sánchez, D.; García-Mateos, G.; Ruiz-Canales, A.; Ferrández-Villena-García, M.; Molina-Martínez, J.M. A Machine Learning Method to Estimate Reference Evapotranspiration Using Soil Moisture Sensors. *Appl. Sci.* **2020**, *10*, 1912. [[CrossRef](#)]
36. Er-Raki, S.; Chehbouni, G.; Hoedjes, J.; Ezzahar, J.; Duchemin, B.; Jacob, F. Improvement of FAO-56 method for olive orchards through sequential assimilation of thermal infrared-based estimates of ET. *Agr. Water Manag.* **2008**, *95*, 309–321. [[CrossRef](#)]
37. Ramos, T.B.; Darouich, H.; Oliveira, A.R.; Farzamian, M.; Monteiro, T.; Nadia Castanheira, N.; Paz, A.; Gonçalves, M.C.; Pereira, L.S. Water use and soil water balance of Mediterranean tree crops assessed with the SIMDualKc model in orchards of southern Portugal. *Agr. Water Manag.* **2023**, *279*, 108209. [[CrossRef](#)]

**Disclaimer/Publisher’s Note:** The statements, opinions and data contained in all publications are solely those of the individual author(s) and contributor(s) and not of MDPI and/or the editor(s). MDPI and/or the editor(s) disclaim responsibility for any injury to people or property resulting from any ideas, methods, instructions or products referred to in the content.